JOC The Journal of Organic Chemistry

Article

pubs.acs.org/joc

The Synthesis and Characterization of Highly Fluorescent Polycyclic Azaborine Chromophores

Carl Jacky Saint-Louis,[†] Lacey L. Magill,[†] Julie A. Wilson,[†] Andrew R. Schroeder,[†,⊥] Sarah E. Harrell,[†] Nicolle S. Jackson,[†] Jamie A. Trindell,[†,¶] Saraphina Kim,[†] Alexander R. Fisch,[†,∥] Lyndsay Munro,[‡] Vincent J. Catalano,[‡] Charles Edwin Webster,[§] Pamela P. Vaughan,[†] Karen S. Molek,[†] Alan K. Schrock,*[,†] and Michael T. Huggins*[,†]

[†]Department of Chemistry, University of West Florida, Pensacola, Florida 32514, United States

[‡]Department of Chemistry, University of Nevada, Reno, Reno, Nevada 89557, United States

[§]Department of Chemistry, Mississippi State University, Mississippi State, Mississippi 39762, United States

[⊥]School of Medicine, University of Alabama, 1825 University Boulevard, Birmingham, Alabama 35294, United States

[¶]Department of Chemistry, University of Texas-Austin, 120 Inner Campus Dr., Austin, Texas 78712, United States

[∥]Department of Chemistry, University of Tennessee, 1420 Circle Dr., Knoxville, Tennessee 37996, United States

Supporting Information

ABSTRACT: Six new heteroaromatic polycyclic azaborine chromophores were designed, synthesized, and investigated as easily tunable high-luminescent organic materials. The impact of the nitrogen-boron-hydroxy (N-BOH) unit in the azaborines was investigated by comparison with their *N*-carbonyl analogs. Insertion of the N-B(OH)-C unit into heteroaromatic polycyclic compounds resulted in strong visible absorption and sharp fluorescence with efficient quantum yields. The solid-state fluorescence of the heteroaromatic polycyclic compounds displayed a large Stokes shift compared to being in solution. The large Stokes shifts observed offset the self-quench effect in the solid state.

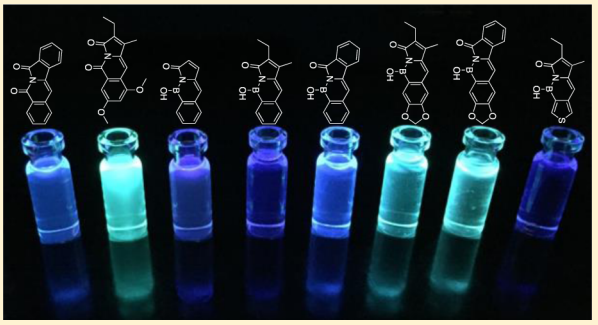

INTRODUCTION

Fluorescent organic compounds have become popular in the materials and imaging technology markets because of their applications in organic field-effect transistors (OFETs), solid-state lasers, biological imaging, organic light-emitting diodes (OLEDs),[1−4] and OLED billboards.[5] OLED materials contain flat structures[6] or heteroaromatic polycyclic molecules with extended conjugated π-systems.[7−10] Heteroaromatic polycyclic compounds are particularly useful because of their simultaneous tunability of fluorescence color and intensity, making them well suited as sensors and fluorophores in bioimaging.[1,11]

Aromatic azaborines are highly regarded because of their fundamental electronic and optical properties which can be beneficial in organic optoelectronic materials.[12] The original aromatic azaborine compounds, 9,10-azaboraphenanthrene and azaboranaphthalene, were synthesized in the late 1950s by Deward and co-workers.[13,14] It was found that the azaborines undergo electrophilic aromatic substitution and possess a high degree of resonance stability.[15−19] In 1960, the first monocylic 1,2-azaborine was prepared and found to be stabilized by the aromaticity of the azaborane ring.[20] In 2000, the Ashe group had a breakthrough in optimizing the synthesis of the 1,2-azaborines by utilizing a ring-closing metathesis/oxidation method.[21−24] Recently, the Liu group showed the preparation of 1,2-azaborines with a variety of substituents (Bu, vinyl, phenylethynyl, NMe_2, SBn, O*t*Bu, H, and OCH_2COOMe) attached to the boron.[25] Based on this new method, the Liu group was able to create a large library of 1,2-azaborine derivatives in good yield. The rich history of azaborines was well documented in a recent review.[26]

The incorporation of various functional groups and heteroatoms in polycyclic aromatic hydrocarbons (PAHs) has been of great interest because they induce modification of the electronic transitions energies in the nonflexible π-systems.[27] For example, the replacement of one of the C−C bonds with an azaborine type B−N bond within the PAH extended conjugation is a well-known method to rigidify the core of a compound.[28] Also, the addition of the B−N bond has been shown to provide more intense fluorescence, extraordinary thermal and photochemical stability, high fluorescence quantum yields,[29,30] and even unique self-assembly behaviors.[31] The B−N bond is also stabilized by the aromaticity of the PAH.[27,32,33]

Recently, a novel PAH was shown to be an effective sensor for the detection of organophosphates (Figure 1). In the study,

Received: August 14, 2016
Published: October 5, 2016

DOI: 10.1021/acs.joc.6b01998
J. Org. Chem. 2016, 81, 10955−10963

Figure 1. Fluorescent *N,N′*-carbonyldipyrrinone for the detection of organophosphates.

an *N,N′*-carbonyldipyrrinone served as the optical core for the sensor molecule, which possessed an appended oximate functional group designed for reaction with the organophosphates. Reaction with the organophosphates changes the color of the *N,N′*-carbonyldipyrrinone fluorescence, providing the sensor functionality.[34]

Replacing the N-C(=O)-N unit (blue) with a N-B(OH)-C unit in the core of the *N,N′*-carbonyldipyrrinone, producing an azaborine, was expected to cause a significant change in the electronic and optical properties of this heteronuclear PAH and increase fluorescence quantum yields. To initiate our investigation, we synthesized a comparison set of heteroaromatic polycyclic compounds where the N-C(=O)-N imide group was replaced with a N-BOH unit to define the structure–property relationships developed by changing the bonding structure in the ring. Based on promising early results, the family of N-BOH heteroaromatics was expanded as shown in Figure 2. Additional substituents were added to the left and right sides of the core structures to define the role of electron-donating substituents on their HOMOs and LUMOs and to aid in understanding fluorescence tunability as shown in Figure 2. Herein, the synthesis and structure–property relationships of novel heteroaromatic polycyclic organic structures containing the N-BOH moiety is presented. Incorporation of the N-BOH group in place of the N-C=O unit generated minimal impact on the UV–vis absorbance, but significantly increased fluorescence efficiency, and increased the Stokes shift of the fluorescence. Altering the left and right sides of the PAH provides a rational route to tunability of these highly efficient fluorescence structures.

SYNTHESIS

In 2004, Boiadjiev and Lightner demonstrated that a base-catalyzed reaction of a pyrrolin-2-one with a pyrrole-2-aldehyde containing a 3-carboethoxy moiety underwent a condensation–intramolecular cyclization to form the pyrrolo[3,2-*f*]indolizine-4,6-dione chromophore in a one-pot synthesis (Figure 3).[35−37]

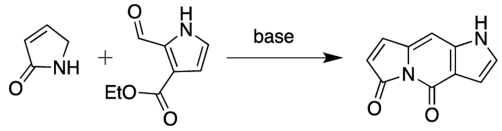

Figure 3. One-pot base-catalyzed condensation–intramolecular cyclization reaction.

Using the same methodology, the reaction of ethyl 2-formylbenzoate **11** and pyrrolin-2-one **12** in refluxing ethanolic DBU yielded imide target **1** (Scheme 1). The reaction of the corresponding pyrrolin-2-one derivatives **13** and **14** with **11** gave imide targets **2** and **3**, respectively. To explore the insertion of the N-BOH unit into the chromophore, (2-formylphenyl)boronic acid **15** was allowed to react under the same conditions with pyrrolin-2-one derivatives **12**, **13**, and **14** to yield azaborines **5**, **6**, and **7**, respectively. The addition of an electron-rich substituent to the right side of the chromophore was performed by the reaction of **13** with **16** to yield imide target **4**, **13** with **17** to yield azaborine **8**, and **14** with **17** to yield azaborine **9** under the same synthetic conditions. Lastly, to interchange the fused-phenyl ring in the right hemisphere with a fused-thiophene, the corresponding pyrrolin-2-one derivative **13** was allowed to react with **19** under the same synthetic conditions yielding azaborine **10**.

RESULTS AND DISCUSSION

X-ray quality crystals of compounds **4** and **6** were obtained by the slow diffusion of hexanes into a saturated chloroform solution at room temperature (21 °C). The molecular structures of **4** and **6** are depicted in Figure 4 as determined by X-ray diffraction. Both molecular structures showed planar molecular core units (Figure 4). The X-ray crystal structure of **6** confirmed the presence of the unusual N-BOH moiety in the chromophore and the planar three-coordinate boron with bonds to C, O, and N (Figure 4B). Furthermore, an intramolecular hydrogen bond between the lactam C=O and the boron O–H was observed in the solid structure of **6** with a H···O distance of 2.23 Å (Figure 4B). The X-ray structure of **6** indicates that electron delocalization consistent with aroma-

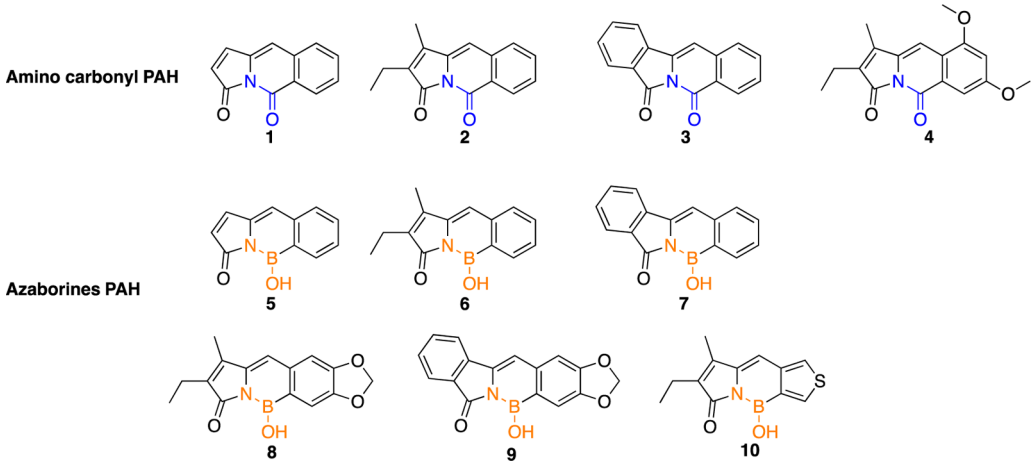

Figure 2. Structures of heteroaromatic polycyclic hydrocarbons; imide in blue, and azaborines in orange.

DOI: 10.1021/acs.joc.6b01998
J. Org. Chem. 2016, 81, 10955−10963

Scheme 1. Synthetic Routes of Compounds 1−10[a]

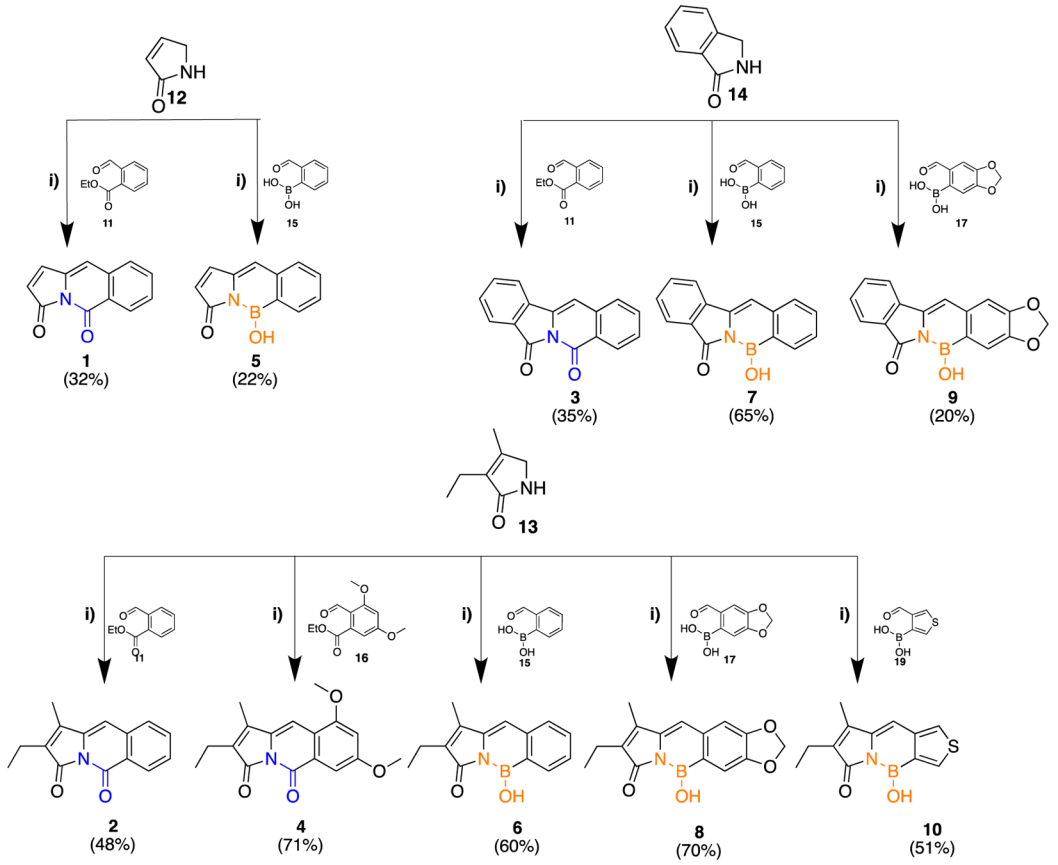

[a]Reagents and conditions: (i) DBU, ethanol (absolute), N_2.

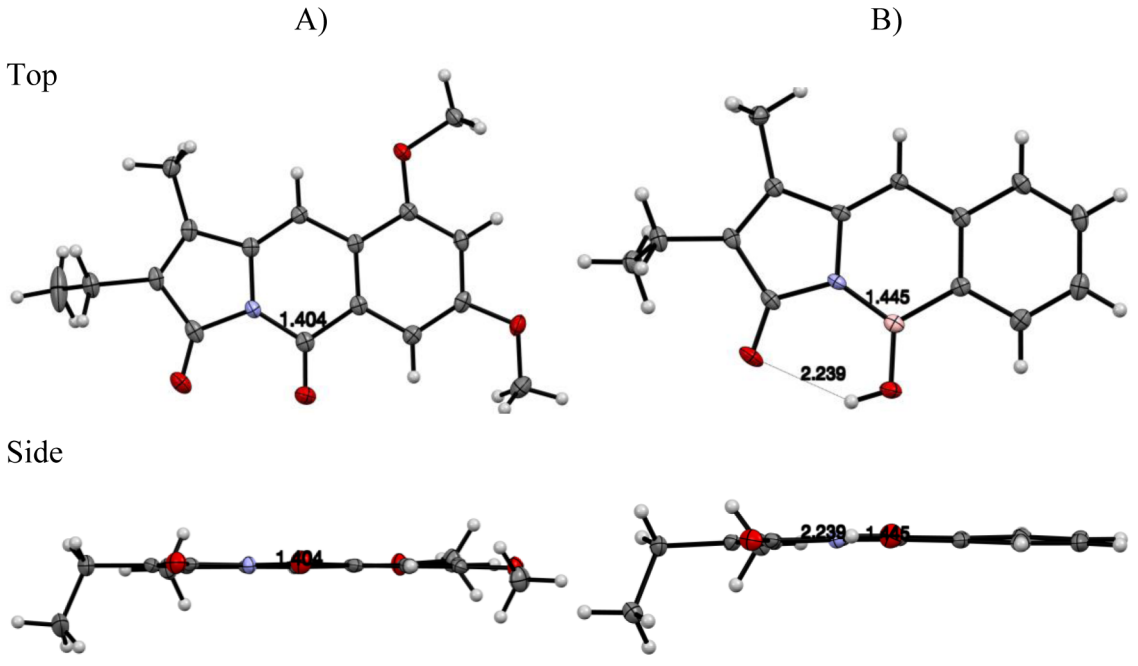

Figure 4. (A) Top and side views of the molecular structure of **4** from X-ray diffraction. (B) Top and side views of the molecular structure of **6** from X-ray diffraction with intramolecular hydrogen bond shown with small dashed line. ORTEP of single molecule with thermal ellipsoids drawn at 50% probability (gray: carbon, red: oxygen; blue: nitrogen; white: hydrogen; pink: boron).

ticity may be present in the central ring containing the B−N unit. This conclusion is based on the length of the B−N bond in **6**, which was measured to be 1.44 Å (Figure 4B) and agrees with the sp^2 type B−N bond length (1.44 Å) seen in borazine.[38−40] However, further studies are needed to confirm aromaticity of the azaborine moiety in this system.

DOI: 10.1021/acs.joc.6b01998
J. Org. Chem. 2016, 81, 10955−10963

Table 1. Experimental UV−vis Absorbance (λ_{max}) and Molar Absorption Coefficient (ε) Data for Target Compounds 1−10 in Various Solvents and Solid-State Excitation (λ_{max})[a]

compds	$CHCl_3$ λ_{max} (ε)[b]	CH_3OH λ_{max} (ε)[b]	DMSO λ_{max} (ε)[b]	CH_3CN λ_{max} (ε)[b]	hexanes λ_{max} (ε)[b]	solid-state excitation λ_{max}
1	353 (5070)	349 (12857)	357 (10590)	351 (7190)	[c]	[d]
2	371 (17300)	370 (11800)	373 (15100)	369 (12900)	366 (13300)	[d]
3	379 (10900)	379 (10900)	382 (11900)	377 (7730)	[c]	436
4	434 (12200)	433 (13000)	434 (16800)	433 (15000)	[c]	476
5	365 (14600)	364 (18100)	364 (18000)	360 (16000)	[c]	409
6	362 (17400)	359 (15700)	361 (10750)	358 (16000	378 (18600)	404
7	375 (18000)	372 (32200)	372 (29100)	371 (20000)	[c]	427
8	389 (10600)	381 (16000)	384 (13300)	383 (13000)	[c]	440
9	397 (6000)	394 (7000)	396 (4800)	392 (3470)	[c]	453
10	355 (24500)	355 (27600)	352 (18100)	350 (25000)	351 (41500)	394

[a] λ_{max} with the highest absorbance in nm. [b] ε is the molar absorptivity in L mol^{-1} cm^{-1} for λ_{max} with the highest absorbance. [c] Absorption could not be obtained because of low solubility in solvent. [d] Excitation maximum could not be obtained in the solid state.

Absorbance. Heteroaromatic polycyclic compounds are well-known to have strong visible absorption and intense fluorescence with efficient quantum yields.[41−43] To broaden the understanding on the optical characteristics of the newly synthesized heteroaromatic polycyclic compounds **1**−**10**, the experimental UV−vis absorbance and molar absorption coefficient were measured in various solvents (Table 1). The solid-state excitation of compounds **1**−**10** are also shown in Table 1.

The azaborines **5**−**7** have similar absorption maxima compared to their imides **1**−**3** in all the selected solvents (Table 1). However, azaborines **5**-**7** displayed higher molar absorptivities than their imides **1**-**3**. Both the azaborines and the imides analogues behave similarly when an electron-donating substituent is introduced to the right hemisphere, resulting in a red-shift of the absorption maximum. This red-shift trend of the absorption maximum can be observed when imide **4** is compared to imide **2**. The same trend can also be observed when azaborine **8** is compared to **6** and azaborine **9** is compared to **7** (Table 1). Furthermore, the addition of a fused-phenyl group to the imide analog **1** red-shifted the absorption maximum of **3**, and the addition of a fused-phenyl group to the azaborines **5** red-shifted the absorption maximum of **7** (Table 1).

The excitation maxima of compounds **3**−**10** in the solid state were considerably red-shifted compared to solution results (Table 1). Compounds **1** and **2** showed minimal excitation and no excitation maxima in the solid state. Among the imide derivatives, compound **3** shows the largest red-shift in the solid state. The excitation maxima of **3** red-shifted from 379 nm in chloroform to 436 nm in the solid state, resulting in a 54 nm red-shift. Among the azaborines, compound **9** shows the largest red-shift when excited in the solid state. The excitation maxima of **9** red-shifted from 397 nm in chloroform to 453 nm in the solid state, resulting in a 56 nm red-shift, while compound **10** shows the smallest red-shift in the excited the solid state. The excitation maxima of **10** red-shifted from 355 nm in chloroform to 394 nm in the solid state, resulting in a 39 nm red-shift. Based on this observation, we assumed that the red-shift in the excitation maxima for compounds **3**−**10** is due to the compact molecular packing in the solid state, resulting from $\pi-\pi$ stacking interactions. This $\pi-\pi$ stacking interaction creates an enlarged network of conjugation in the solid state, resulting in the large red-shifts observed in the solid state compared to the solution results.

The electronic structure of the azaborines and their resulting optical properties can be explained using a two hemisphere model of azaborine **5**. Figure 5 displays the two hemispheres,

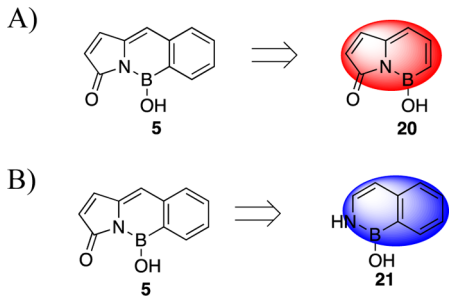

Figure 5. (A) Left hemisphere (red) of **5** responsible for an absorbance near 348 nm. (B) Right hemisphere (blue) of **5** responsible for an absorbance near 251 nm.

with left hemisphere in red and the right hemisphere in blue. The pyrrol-2- one and the azaborine ring make up the left hemisphere **20** (Figure 5A); the fused-phenyl and the azaborine ring make up the right hemisphere **21** (Figure 5B) of the molecule.

The molecular geometry of the two hemispheres in the ground state was fully optimized using density functional theory (DFT) at the B3LYP/6-311+G** level. The B3LYP/6-311+G** calculated energies of HOMO, LUMO, and band gap are −6.60, −3.04, and 3.56 eV, respectively, for the left hemisphere**20**, which correspond to a 348 nm absorbance (Table S1). The B3LYP/6-311+G** calculated energies of HOMO, LUMO, and band gap are −5.74, −0.80, and 4.94 eV, respectively for the right hemisphere **21** (Table S1). The band gap energy calculated for the right hemisphere corresponded to a 251 nm absorbance, similar to that of a naphthalene derivative.[44] This result indicates that the left hemisphere functions as the optical core in **5** and is responsible for the absorbance in the ranges of 348−390 nm found for **5**−**10**. These results also show that the boron orbitals are included in the extended ring conjugation. Simulated UV−vis spectra of **20** and **21** were also computed in the gas phase (see Supporting Information). The calculations also revealed that the left hemisphere, **20**, is responsible for the absorbance near 348 nm and the right hemisphere, **21**, corresponded to 251 nm absorbance.

DOI: 10.1021/acs.joc.6b01998
J. Org. Chem. 2016, 81, 10955−10963

Table 2. Emission λ Max and Quantum Yield for Compounds 1−10 in Various Solvents and in the Solid State

compds	$CHCl_3$ λ_{em}[a] (Φ_F)	CH_3OH λ_{em}[a] (Φ_F)	DMSO λ_{em}[a] (Φ_F)	CH_3CN λ_{em}[a] (Φ_F)	hexanes λ_{em}[a] (Φ_F)	solid-state emission λ_{em}[a]
1	410 (0.29)	450 (0.53)	420 (0.43)	410 (0.50)	[b]	520
3	445 (0.18)	445 (0.02)	455 (0.12)	(443) (0.16)	[b]	489
4	469 (0.60)	510 (0.44)	485 (0.60)	476 (0.54)	[b]	510
5	420 (0.65)	416 (0.10)	430 (0.01)	412 (0.97)	[b]	459
6	418 (0.36)	411 (0.12)	416 (0.19)	411 (0.42)	405 (0.25)	468
7	437 (1.00)	430 (0.74)	438 (0.12)	432 (0.97)	[b]	474
8	474 (0.61)	484 (0.30)	498 (0.80)	488 (0.57)	[b]	490
9	474 (0.65)	490 (0.57)	500 (0.05)	490 (0.63)	[b]	502
10	414 (0.20)	418 (0.35)	425 (0.87)	412 (0.97)	396 (0.18)	465

[a] λ_{em} is the lambda max of the fluorescence in nm; Φ_F is the quantum yield. [b] Fluorescence could not be observed. Note that the amino carbonyl 2 was omitted because no fluorescence was detected in any of the selected solvents or in the solid state.

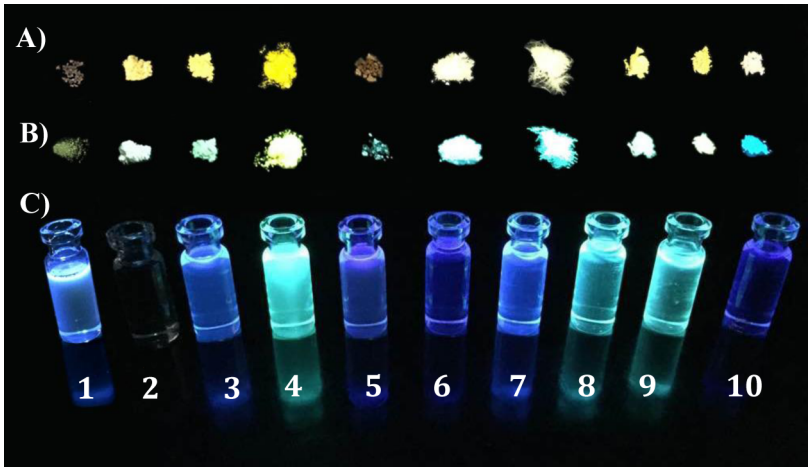

Figure 6. (A) Photo of solid PAHs **1**−**10** (from left to right) in normal room lighting. (B) Photo of solid fluorescence of **1**-**10** (from left to right) taken in the dark under a hand-held UV (365 nm) lamp. (C) Photo of fluorescence of **1**−**10** (from left to right) in chloroform taken in the dark under a hand-held UV (365 nm) lamp.

The addition of a fused-phenyl ring to the left hemisphere of **5** increases the conjugation and raises the HOMO energy, resulting in a red-shift in absorbance as shown for **7** (Table S1). The addition of an electron-donating substituent to the right hemisphere also raises the HOMO energy, resulting in a red-shift in absorbance as in the case of **8** and **9**. Surprisingly, the addition of an electron-rich moiety to the left hemisphere of **5** did not have a significant effect on the HOMO or LUMO energies or the absorbance as in the case of **6**. Lastly, to validate that the right hemisphere is not the optical core responsible for the absorbances near 348−390 nm, we altered the right hemisphere of **6** experimentally by replacing the fused-phenyl ring with a fused-thiophene ring. We expected that the fused-thiophene ring would perform as an electron-rich ring and red-shift the absorbance range of the optical core of **6**. The fused-thiophene ring instead behaved as an electron-withdrawing substituent on the optical core, raising the LUMO energy and blue shifting the absorbance of **10** as compared to **6** by 7 nm from 362 to 355 nm, consistent with the HOMO−LUMO computational results (Table S1). Similar to **20** and **21**, the simulated UV−vis spectra for compounds **1**−**10** were computed in the gas phase to support our findings (see Supporting Information). The gas-phase computations for compounds **1**−**10** were also consistent with the observed experimental absorbances.

Fluorescence. The emission spectra of compounds **1**−**10** were measured against coumarin 153 or 9,10-diphenylanthracene as standard references. Table 2 shows the emission maxima and the quantum yields of all the heteroaromatic polycyclic compounds in various solvents and the emission maxima in the solid state. Compound **2** did not show any emission in solution or in the solid state. The fluorescence in solution of the imide derivatives **1**, **3**, and **4** was compared to the fluorescence of the azaborines **5**−**10**. In solution, azaborines **5**−**7** exhibited quantum yields approximately five times higher than that of **3** (Table 2). However, the quantum yield of compound **4** is comparable to that of azaborine **8**. The replacement of the imide unit of compound **2** with the N-BOH unit resulted in an emission for **6** in all the selected solvents, while no emission was detected for **2**. Azaborine **5** displayed higher quantum yields than its amino carbonyl precursor **1** in chloroform and acetonitrile (Table 2). Azaborine **7** displayed higher quantum yields than its amino carbonyl precursor **3** in all the selected solvents (Table 2). Computations have shown that the empty p-orbital of a tricoordinate boron center will overlap with an adjacent organic π-systems or heteroatom such as oxygen and nitrogen leading to strong photoluminescence,[45] and we proposed that the same effect is seen here with these azaborines.

The addition of an electron-donating moiety to the right hemisphere of the azaborine derivatives resulted in a red shift of the emission maximum and raised the HOMO energy. For example, the addition of an acetal group to the right hemisphere of **6** resulted in a red shift of the emission maximum from 418 to 474 nm in chloroform as seen in the comparison of **6** and **8** (Table 2). Similar results were observed

DOI: 10.1021/acs.joc.6b01998
J. Org. Chem. 2016, 81, 10955−10963

for **9**, the addition of acetal group to **7** also resulted in a red shift of the emission maximum from 437 to 474 nm in chloroform (Table 2).

The addition of a phenyl group to the left hemisphere of **5** resulted in a red shift of the emission maximum as seen in the comparison of **5** and **7** (Table 2). Surprisingly, the addition of an electron-donating substituent to the left hemisphere of **5** did not have a significant effect on the emission maximum as seen in the comparison of **5** and **6** (Table 2). To further demonstrate that the right hemisphere is not the optical core responsible for the fluorescence of the azaborines, the right hemisphere of **6** was altered by replacing the fused-phenyl ring with a fused-thiophene ring. We expected that the emission of compound **10** would be red-shifted because of the electron-rich nature of the thiophene ring. However, an emission maximum similar to that of **6** was observed for **10** in all selected solvents (Table 2).

A pictorial representation under a hand-held UV (365 nm) lamp of the emission of compounds **1**−**10** in chloroform is displayed in Figure 6C. No fluorescence was detected for the amino carbonyl compound **2** in solution.

The Stokes shift of azaborines **5**−**10** was determined in chloroform to improve understanding of the effect of the substituent on the hemispheres of **5** (Table S2). The emission maximum of **5** was at 420 nm in chloroform with a 55 nm Stokes shift. The addition of an electron-donating substituent to the left hemisphere of **5** did not change the Stokes shift as shown for **6** with an emission maximum of 418 nm in chloroform with a 56 nm Stokes shift. The addition of a fused-phenyl group to the left hemisphere of **5** increased the Stokes shift by 7 nm as seen for **7**. The emission maximum of **7** was at 437 nm in chloroform with a 62 nm Stokes shift.

Azaborines containing electron-donating substituents on the right hemisphere exhibited the largest Stokes shifts. The addition of an acetal group to the right hemisphere of **6** increased the Stokes shift by 29 nm in chloroform as seen for **8**. The emission maximum of **8** was at 474 nm in chloroform with an 85 nm Stokes shift. Similarly, the addition of an acetal group to the right hemisphere of **7** increased the Stokes shift by 15 nm in chloroform as seen for **9**. The emission maximum of **9** was at 474 nm in chloroform with a 77 nm Stokes shift. The replacement of the fused-phenyl group of **6** by a fused-thiophene group on the right hemisphere did not have a significant effect on the emission as seen for **10**. The emission maximum of **10** was at 414 nm in chloroform with a 59 nm Stokes shift. The simulated emission spectra of compounds **1**−**10** in the gas phase were computed and compared to their simulated UV−vis spectra (see Supporting Information). The Stokes shifts observed experimentally were consistent with the computations in the gas phase.

A red-shift in emission maximum was observed for all of the heteroaromatic polycyclic compounds, **1**−**10** with the exception of **2**, in the solid state. Among the imide derivatives, compound **1** showed the largest red-shift. The emission maximum of **1** red-shifted from 410 nm in chloroform to 520 nm in the solid state, resulting in a 110 nm red-shift (Table 2). Among the azaborine derivatives, compounds **6** and **10** showed the largest red-shift in the solid state, while compound **8** showed the smallest red-shift in the solid state. Based on this observation, we believe that the large Stokes shift observed in the solid state can offset the self-quench effect. Furthermore, the more compact molecular packing in the solid state can result in $\pi-\pi$ stacking and promotes a red shift in the emission.[46] See Supporting Information for the normalized emission spectra of **1**−**10** in the solid state.

CONCLUSIONS

In summary, six heteroaromatic polycyclic azaborine compounds were designed and synthesized along with four of their carbonyl containing analogs. Molecular structures determined by X-ray diffraction of the azaborines showed planar molecular core units, confirmed the presence of the unusual N-BOH moiety, and confirmed the aromaticity of the central ring containing the N-BOH unit.

The optical measurements of the heteroaromatic polycyclic compounds indicated that the azaborines have similar absorption maxima compared to their carbonyl analogs. However, the majority of the azaborines exhibited a higher molar absorption coefficient than their carbonyl analogs. The azaborines exhibited high emission quantum yields compared to the imide analogs. Addition of electron-donating substituents on the right hemisphere increased the HOMO energies and resulted in red-shifted absorbance and emission maxima, while electron-donating substituents on the left hemisphere resulted in little change in HOMO−LUMO energies and optical properties. The change in HOMO−LUMO energies caused by the addition of substituents on the right and left side of the azaborines enabled a rational tuning of fluorescence maxima.

EXPERIMENTAL SECTION

General Methods. Starting materials and solvents were purchased from commercial suppliers unless noted otherwise. Compound **12** was synthesized according to the literature procedures.[47] ^{1}H NMR spectra were recorded at 400 MHz, ^{13}C spectra at 100 MHz, and ^{11}B spectra (sodium tetraphenylborate as standard) at 128 MHz. All chemical shifts are reported in ppm downfield from TMS (δ = 0.00) for ^{1}H NMR and relative to the central $CDCl_3$ (δ = 77.16) for ^{13}C NMR.

Computational Details. Molecular modeling to determine the HOMO and LUMO energies at the B3LYP/6-311+G** was performed with Spartan 14.[48] The theoretical calculations for excitation and emission spectra were carried out using the Gaussian 09[49] implementations of B3LYP (the B3 exchange functional[50] and LYP correlation functional)[51] DFT,[52] using the default pruned fine grids for energies (75, 302), default pruned coarse grids for gradients and Hessians (35, 110), and nondefault SCF convergence for geometry optimizations (10^{-6}). Using the gas-phase optimized geometries, vertical transitions in the UV−vis region were computed with time-dependent DFT (TDDFT)[53] to generate the simulated absorption spectra. For TDDFT single points, the first 50 singlet excitations were solved iteratively [TD(ROOT = *X*, NSTATES = 50) where *X* is the root number, *X* = 1] with the default convergence criteria for the energy (10^{-6}) and nondefault convergence criteria for the wave function (10^{-6}). For TDDFT[5] geometry optimizations, the first singlet excited states were optimized using analytical gradients,[54,55] and the first 30 singlet excitations were solved iteratively [TD(ROOT = 1, NSTATES = 30). All Gaussian 09 computations used the 6-31G(d′) basis sets[56−58] for all atoms. Spherical harmonic *d* functions were used throughout, i.e., there are five angular basis functions per *d* function. All B3LYP/6-31G(d′) structures were fully optimized, and analytical frequency calculations were performed on all ground-state structures to ensure either a zeroth-order saddle point (a local minimum) was achieved. The computationally derived absorption and emission spectra were simulated with an in-house Fortran program by convoluting[59] the computed excitation energies and computed oscillator strengths with a Gaussian line-shape and a broadening of 25 nm.

Synthesis Protocols. *Synthesis of Pyrrolo[1,2-b]isoquinoline-3,5-dione (1).* The pyrrolin-2-one (0.596 g, 7.18 mmol) and methyl 2-formylbenzoate (0.943 g, 5.74 mmol) were combined in a round-bottom flask. The system was flushed with N_2 gas. Ethanol (200 proof,

DOI: 10.1021/acs.joc.6b01998
J. Org. Chem. 2016, 81, 10955−10963

40 mL) was added to the reaction mixture. The solution was stirred at rt until all the materials were completely dissolved resulting in a light-brown solution. DBU (4.29 mL, 28.72 mmol) was added, causing the reaction mixture to become dark brown. The reaction mixture was refluxed under N_2 atmosphere for 24 h. After the 24 h, the dark-brown solution was allowed to cool, and HCl (1 N, 80 mL) was added in 5 mL portions while stirring until a dark-brown precipitate formed. The reaction mixture was cooled below 0 °C for 12 h. After cooling period, the light-brown precipitate was collected and recrystallized in 75% methanol yielding **1** as dark-brown solid 32% (0.364 g, 1.85 mmol). Mp 197 °C (Decomposed); ^{1}H NMR (400 MHz, $CDCl_3$, 25 °C): δ (ppm) 8.46 (d, J = 8.00 Hz, 1H), 7.71, (t, J = 7.19 Hz, 1H), 7.60 (m, 3H), 7.41 (d, J = 16.44 Hz 1H), 6.74 (s, 1H); ^{13}C NMR (100 MHz, DMSO, 25 °C): δ (ppm) 166.3, 162.5, 137.8, 137.3, 135.5, 133.3, 128.5, 127.8, 127.3, 126.9, 120.3, 111.4; IR (ATR) (cm^{-1}): 1712 (m), 1635 (s), 1596 (m), 1553 (w), 1450 (w), 1338 (w), 1295 (w), 1265 (m), 1196 (s), 1153 (m), 1041 (w), 976 (m), 881 (m), 761 (m); HRMS (Magnetic Sector, EI 35 eV) m/z [M]$^{\bullet+}$ calcd for $C_{12}H_7NO_2$ 197.0477, found 197.0482.

*Synthesis of 2-Ethyl-1-methylpyrrolo[1,2-b]isoquinoline-3,5-dione (**2**).* 3-Ethyl-4-methyl-3-pyrrolin-2-one (0.297 g, 2.37 mmol) and methyl 2-formylbenzoate (0.311 g, 1.90 mmol, 264 μL) were dissolved in ethanol (200 proof, 15 mL) under N_2 atmosphere. DBU (1.44 g, 9.48 mmol, 1416 μL) was then added to the mixture resulting in a yellow solution. The reaction mixture was refluxed for 24 h under N_2 atmosphere. After 24 h, the mixture was cooled to rt, then it was placed in an ice bath for 20 min until a yellow precipitate formed. HCl (10 mL, 1 N) was added to the mixture, then it was cooled below 0 °C for 2 h allowing more precipitate to be formed. The yellow precipitate formed was collected via vacuum filtration yielding **2** as yellow crystals 48% yield (0.212g, 0.91 mmol). Mp 190−195 °C; ^{1}H NMR (400 MHz, $CDCl_3$, 25 °C): δ (ppm) 8.43 (d, J = 7.58 Hz, 1H), 7.63, (t, J = 7.32 Hz, 1H), 7.48 (m, 2H), 6.53 (s, 1H), 2.45 (d, q = 7.43 Hz, 2H), 2.19 (s, 3H), 1.16 (t, J = 7.43 Hz, 3H); ^{13}C NMR (100 MHz, $CDCl_3$, 25 °C): δ (ppm) 168.0, 158.5, 141.3, 138.9, 135.4, 134.8, 133.6, 129.3, 128.5, 128.4, 127.6, 104.4, 16.8, 13.0, 9.6; IR (ATR) (cm^{-1}): 1740 (s), 1678 (m), 1644 (m), 1598 (w), 1482 (w), 1380 (m), 1305 (s), 1132 (m), 1098 (w), 1028 (w), 929 (w), 862 (m), 777 (m), 763 (m), 690 (m); HRMS (Magnetic Sector, EI 35 eV) m/z [M]$^{\bullet+}$ calcd for $C_{15}H_{13}NO_2$ 239.0946, found 239.0941.

*Synthesis of Isoindolo[2,1-b]isoquinoline-5,7-dione (**3**).* Isoindolin-1-one (0.152 g, 1.14 mmol) and ethanol (200 proof, 10 mL) were placed in a 25 mL round-bottom flask and stirred at rt under N_2 atmosphere. Once dissolved, methyl 2- formylbenzoate (0.150 g, 0.914 mmol) was added to the reaction flask followed by DBU (0.695 g, 4.57 mmol), which resulted in a cloudy yellow mixture. The mixture was refluxed for 24 h under N_2 atmosphere. The mixture turned clear yellow within the first 10 min of refluxing and red within the first few h. After 24 h of refluxing, the reaction mixture was cooled to rt, and the flask was placed into an ice bath. To the mixture, HCl (1 N, 50 mL) was added until a yellow precipitate formed. The mixture was cooled below 0 °C for 24 h. The yellow precipitate was collected by vacuum filtration and washed with HCl (1 N, 1 mL) and ice-cold water (5 mL) yielding **3** as a yellow solid 21% (0.05 g, 0.20 mmol). Mp 278−280 °C; ^{1}H NMR (400 MHz, $CDCl_3$, 25 °C): δ (ppm) 8.47 (d, J = 7.95 Hz, 1H), 7.97 (d, J = 7.95 Hz, 1H), 7.78 (d, J = 7.95 Hz, 1H), 7.68 (m, 2H), 7.50 (m, 3H), 6.95(s, 1H); ^{13}C NMR (100 MHz, $CDCl_3$, 25 °C): δ (ppm) 165.1, 159.7, 135.6, 135.2, 135.1, 134.7, 133.9, 130.5, 129.5, 128.5, 128.3, 127.8, 127.5, 125.6, 120.5, 103.5; IR (ATR) (cm^{-1}): 1707 (s), 1654 (w), 1616 (w), 1472 (m), 1406 (m), 1353 (m), 1318 (m), 1245 (m), 1137 (m), 1119 (m), 1039 (s), 955 (m), 713 (s); HRMS (Magnetic Sector, EI 35 eV) m/z [M]$^{\bullet+}$ calcd for $C_{16}H_9NO_2$ 247.0633, found 247.0630.

*Synthesis of 2-Ethyl-7,9-dimethoxy-1-methylpyrrolo[1,2-b]-isoquinoline-3,5-dione (**4**).* The 3-ethyl-4-methyl-3-pyrrolin-2-one (0.27 g, 2.17 mmol), methyl 2-formyl- 3,5-dimethoxybenzoate (0.387 g, 1.73 mmol), and ethanol (200 proof, 11 mL) were combined in a 25 mL round-bottom flask and stirred under N_2 atmosphere at rt. DBU (1.32 g, 8.67 mmol) was added to the mixture resulting in a cloudy yellow liquid. The reaction mixture was refluxed under N_2 atmosphere for 22 h. The mixture turned clear yellow within the first 10 min of refluxing and dark orange at the end of refluxing. After refluxing for 22 h, the mixture was cooled to rt and then placed in an ice bath, which resulted in the formation of an orange precipitate. HCl (10 mL, 1 N) was added until more precipitate formed. The mixture was chilled below 0 °C for 3 h. The precipitate was collected by vacuum filtration and washed with HCl (1 N), yielding **4** as an orange solid 71% (0.367 g, 1.23 mmol). X-ray quality crystals of **4** were obtained by the slow diffusion of hexanes into a saturated chloroform solution at rt (21 °C). Mp 197−199 °C; ^{1}H NMR (400 MHz, $CDCl_3$, 25 °C): δ (ppm) 7.48 (s, 1H), 6.84 (s, 1H), 6.66 (s, 1H), 3.90(s, 6H), 2.42 (q, J = 7.77 Hz, 2H), 2.16 (s, 3H), 1.13 (t, J = 7.8 Hz, 3H); ^{13}C NMR (100 MHz, $CDCl_3$, 25 °C): δ (ppm) 168.4, 160.9, 158.3, 156.8, 142.0, 135.9, 132.9, 130.7, 119.9, 103.9, 102.4, 99.3, 55.9, 55.9, 16.7, 13.1, 9.6; IR (ATR) (cm^{-1}): 1742 (s), 1672 (w), 1641 (m), 1610 (m), 1574 (w), 1489 (m), 1458 (m), 1422 (w), 1359 (s), 1296 (s), 1204 (s), 1150 (m), 1068 (m), 1042 (m), 929 (w), 873 (w), 829 (m), 787 (m); HRMS (Magnetic Sector, EI 35 eV) m/z [M]$^{\bullet+}$ calcd for $C_{17}H_{17}NO_4$ 299.1158, found 299.1161.

*Synthesis of 5-Hydroxybenzo[c]pyrrolo[2,1-f][1,2]azaborinin-3(5H)-one (**5**).* The pyrrolin-2-one (0.227 g, 2.73 mmol) and 2-formylphenylboronic acid (0.328 g, 2.19 mmol) were combined in a round-bottom flask. The system was flushed with N_2 gas. Ethanol (200 proof, 10 mL) was added to the reaction mixture. The solution was stirred at rt until all the materials were completely dissolved, resulting in a yellow clear solution. DBU (1.64 mL, 10.92 mmol) was added, causing the reaction mixture to become brown. The reaction mixture was refluxed under N_2 atmosphere for 24 h. After 24 h, the dark-brown solution was allowed to cool, and HCl (1 N, 30.00 mL) was added in 5.00 mL portions while stirring until a light-brown precipitate formed. The reaction mixture was cooled below 0 °C for 12 h. After cooling period, the light-brown precipitate was collected by vacuum filtration, yielding **5** as light-brown solid 22% (0.095 g, 0.482 mmol). Mp 84−89 °C; ^{1}H NMR (400 MHz, $CDCl_3$, 25 °C): δ (ppm) 8.12 (d, J = 7.3 Hz, 1H), 7.65 (s, 1H), 7.54 (t, J = 7.3 Hz, 1H), 7.43 (m, 2H), 7.35 (d, J = 5.5 Hz, 1H), 6.49 (s, 1H), 6.23 (d, J = 5.5 Hz, 1H); ^{13}C NMR (100 MHz, CDCl3, 25 °C): δ (ppm) 177.7, 168.5, 141.5, 140.9, 138.3, 133.5, 132.1, 129.0, 127.9, 124.3, 113.9; ^{11}B NMR (sodium tetraphenyl borate as standard, 128 MHz, acetone-d_6, 25 °C): δ(ppm) 29.46; IR (ATR) (cm^{-1}): 1690 (s), 1638 (w), 1599 (w), 1479 (w), 1451 (m), 1402 (m), 1342 (s), 1297 (m), 1160 (m), 1093 (m), 1005 (m), 847 (m), 812 (m), 759 (m), 693 (m), 608 (s); HRMS (Magnetic Sector, EI 35 eV) m/z [M]$^{\bullet+}$ calcd for $C_{11}H_8BNO_2$ 197.0648, found 197.0647.

*Synthesis of 2-Ethyl-5-hydroxy-1-methylbenzo[c]pyrrolo[2,1-f]-[1,2]azaborinin-3(5H)-one (**6**).* 3-Ethyl-4-methyl-3-pyrrolin-2-one (0.325 g, 2.60 mmol) and 2- formylphenylboronic acid (0.311 g, 2.07 mmol) were combined in a round-bottom flask. The system was flushed with N_2 gas. Ethanol (200 proof, 10 mL) was added to the reaction mixture. The solution was stirred at rt until all the materials were completely dissolved. DBU (1.50 mL) was added, resulting in a color change to pale yellow. The reaction mixture was refluxed under N_2 atmosphere for 24 h. After 24 h, the reaction was cooled to rt and then placed in an ice bath. The reaction was stirred while concentrated HCl (10 mL, 1 N) was added dropwise. A white precipitate formed. The reaction mixture was cooled below 0 °C for 1 h. The precipitate was collected by vacuum filtration, yielding **6** as off-white crystals 60% (0.296 g, 1.24 mmol). X-ray quality crystals of 6 were obtained by the slow diffusion of hexanes into a saturated chloroform solution at rt (21 °C). Mp 118−120 °C; ^{1}H NMR (400 MHz, $CDCl_3$, 25 °C): δ (ppm) 8.07 (d, J = 7.2 Hz, 1H), 7.62 (s, 1H), 7.51 (dd J = 8.1 Hz, 1H), 7.41 (d, J = 8.1 Hz, 1H), 7.35 (t, J = 7.8 Hz, 1H), 6.39 (s, 1H), 2.38 (q, J = 7.5 Hz, 2H), 2.14 (s, 3H), 1.13(dd, J = 8.1 Hz, 3H); ^{13}C NMR (100 MHz, $CDCl_3$, 25 °C): δ (ppm) 177.7, 145.0, 141.2, 139.2, 134.5, 133.3, 131.9, 128.4, 127.1, 108.5, 16.5, 13.1, 9.7; ^{11}B NMR (sodium tetraphenyl borate as standard, 128 MHz, acetone-d_6, 25 °C): δ(ppm) 29.36; IR (ATR) (cm^{-1}): 3466 (w), 1681 (s), 1635 (m), 1451 (m), 1396 (m), 1357 (m), 1338 (m), 1295 (w), 1165 (w), 1105 (m), 1081 (w), 1013 (m), 955 (w), 908 (m), 791 (m), 756 (m), 697 (m), 619

DOI: 10.1021/acs.joc.6b01998
J. Org. Chem. 2016, 81, 10955−10963

(m); HRMS (Magnetic Sector, EI 35 eV) m/z $[M]^{\bullet+}$ calcd for $C_{14}H_{14}BNO_2$ 239.1118, found 239.1120.

*Synthesis of 5-Hydroxybenzo[3,4][1,2]azaborinino[6,1-a]-isoindol-7(5H)-one (**7**).* Isoindolin-1-one (1.00 g, 7.50 mmol) and 2-formylphenylboronic acid (0.90 g, 6.00 mmol) were combined in a round-bottom flask. The system was flushed with N_2 gas. Ethanol (30 mL, 200 proof) was added to the reaction mixture. The solution was stirred at rt until all the materials were completely dissolved. DBU (4.50 mL) was added, resulting in a color change to bright yellow. The reaction mixture was refluxed under N_2 atmosphere for 24 h. After 24 h, the reaction was cooled to rt and then placed in an ice bath. The reaction was stirred while HCl (20 mL, 1 N) was added dropwise. Yellow precipitate formed. The reaction mixture was cooled below 0 °C for 2 h. The precipitate was collected by vacuum filtration and recrystallized in 75% EtOH yielding **7** as bright yellow crystals 65% (1.11 g, 4.50 mmol). Mp 185−188 °C; ^{1}H NMR (400 MHz, $CDCl_3$, 25 °C): δ (ppm) 8.16 (d, J = 7.5 Hz, 1H), 7.98 (s, 1H), 7.91 (d, J = 7.5 Hz, 1H), 7.79 (d, J = 7.8 Hz, 1H), 7.67 (t, J = 7.5 Hz, 1H), 7.58 (t, J = 7.5 Hz, 1H), 7.50 (d, J = 7.8 Hz, 1H), 7.49 (t, 1H), 7.40 (t, J = 7.5 Hz, 1H), 6.85 (s, 1H); ^{13}C NMR (100 MHz, $CDCl_3$, 25 °C): δ (ppm) 174.8, 141.4, 139.0, 134.7, 134.1, 133.4, 132.3, 129.4, 129.3, 128.1, 127.0, 124.8, 120.5, 107.3, 77.2; ^{11}B NMR (sodium tetraphenyl borate as standard, 128 MHz, acetone-d_6, 25 °C): δ (ppm) 30.45; IR (ATR) (cm^{-1}): 1692 (m), 1651 (m), 1613 (w), 1472 (w), 1384 (m), 1359 (m), 1285 (w), 1200 (w), 1137 (m), 1112 (m), 1084 (m), 961 (m), 762 (m), 712 (s); HRMS (Magnetic Sector, EI 35 eV) m/z $[M]^{\bullet+}$ calcd for $C_{15}H_{10}BNO_2$ 247.0805, found 247.0810.

*Synthesis of 8-Ethyl-5-hydroxy-9-methyl-[1,3]dioxolo[4′,5′:4,5]-benzo[1,2-c]pyrrolo[2,1-f][1,2]azaborinin-7(5H)-one (**8**).* The 3-ethyl-4-methyl-3-pyrrolin-2- one (0.25 g, 1.99 mmol) and 2-formyl-4,5-methylenedioxyphenylboronic acid (0.309g, 1.59 mmol) were combined in a round-bottom flask. The system was flushed with N_2 gas. Ethanol (200 proof, 10 mL) was added to the reaction mixture. The solution was stirred at rt until all the materials were completely dissolved. DBU (1.21 g, 7.98 mmol) was added to the mixture, resulting in a color change to a yellow solution. The reaction mixture was refluxed under N_2 atmosphere for 24 h. After 24 h, the reaction was cooled to rt then placed in an ice bath. The reaction was stirred while HCl (1 N) was added dropwise. After the precipitate formed, the reaction mixture was cooled below 0 °C for 1 h. The precipitate was collected by vacuum filtration, yielding **8** (70%, 0.31 g, 1.11 mmol) as a yellow solid. Mp 161−165 °C; ^{1}H NMR (400 MHz, $CDCl_3$, 25 °C): δ (ppm) 7.49 (s, 1H), 7.45 (s, 1H), 6.85 (s, 1H), 6.27 (s, 1H), 6.01 (s, 2H), 2.37 (q, J = 7.8 Hz, 2H,), 2.12 (s, 3H), 1.12 (t, J = 7.8 Hz, 3H); ^{13}C NMR (100 MHz, $CDCl_3$, 25 °C): δ (ppm) 177.9, 151.0, 147.4, 145.1, 138.2, 137.5, 133.7, 111.8, 108.2, 108.1, 101.3, 16.5, 13.2, 9.7; ^{11}B NMR (sodium tetraphenyl borate as standard, 128 MHz, acetone-d_6, 25 °C): δ (ppm) 28.87; IR (ATR) (cm^{-1}): 1679 (s), 1651 (w), 1500 (w), 1482 (w), 1401 (w), 1331 (m), 1238 (s), 1144 (m), 1032 (s), 957 (w), 932 (m); HRMS (Magnetic Sector, EI 35 eV) m/z $[M]^{\bullet+}$ calcd for $C_{15}H_{14}BNO_4$ 283.1016, found 283.1018.

*Synthesis of 5-Hydroxy[1,3]dioxolo[4″,5″:4′,5′]benzo[1′,2′:3,4]-[1,2]azaborinino[6,1-a]isoindol-7(5H)-one (**9**).* Isoindolin-1-one (0.17 g, 1.31 mmol) and 2- formyl-4,5-methylenedioxyphenyl boronic acid (0.20 g, 1.05 mmol) were combined in a round-bottom flask. The system was flushed with N_2 gas. Ethanol (200 proof, 10 mL) was added to the reaction mixture. The solution was stirred at rt until all the materials were completely dissolved. DBU (783 μL) was added to the mixture, resulting in a color change to a yellow solution. The reaction mixture was refluxed under N_2 atmosphere for 24 h. After 24 h, the reaction was cooled to room temperature and then placed in an ice bath. The reaction was stirred while HCl (1 N, 20 mL) was added dropwise. After the precipitate formed, the reaction mixture was cooled below 0 °C for 1 h. The precipitate was collected by vacuum filtration yielding **9** as a yellow solid 20% (0.61g, 0.21 mmol). Mp 215−218 °C; ^{1}H NMR (400 MHz, $CDCl_3$, 25 °C): δ (ppm) 7.85 (d, J = 7.7 Hz, 1H), 7.79 (s, 1H), 7.70 (d, J = 7.7 Hz, 1H), 7.62 (t, J = 7.7 Hz, 1H), 7.49 (s, 1H), 7.43(t, J = 7.7 Hz, 1H), 6.90 (s, 1H), 6.68 (s, 1H), 6.02 (s, 2H); ^{13}C NMR (100 MHz, $CDCl_3$, 25 °C): δ (ppm) 174.8, 151.4, 147.4, 139.0, 137.8, 134.0, 133.7, 129.1, 129.0, 124.8, 120.2, 111.7, 107.7, 107.1, 101.3; ^{11}B NMR (sodium tetraphenyl borate as standard, 128 MHz, acetone-d_6, 25 °C): δ (ppm) 30.43; IR (ATR) (cm^{-1}): 1708 (s), 1652 (w), 1613 (w), 1476 (m), 1406 (m), 1357 (m), 1318 (m), 1244 (m), 1135 (m), 1118 (m), 1037 (s), 956 (m), 752 (m), 714 (s); HRMS (Magnetic Sector, EI 35 eV) m/z $[M]^{\bullet+}$ calcd for $C_{16}H_{10}BNO_4$ 291.0703, found 291.0711.

*Synthesis of 7-Ethyl-4-hydroxy-8-methyl-4H,6H-pyrrolo[2,1-f]-thieno[3,4- c][1,2]azaborinin-6-one (**10**).* The 3-ethyl-4-methyl-3-pyrrolin-2-one (0.31g, 2.50 mmol) and 4-formylthiophenboronic acid (0.31 g, 2.00 mmol) were combined in a round-bottom flask. The system was flushed with N_2 gas. Ethanol (10 mL, 200 proof) was added to the reaction mixture. The solution was stirred at rt until all materials were completely dissolved, resulting in a yellow solution. DBU (1.50 mL, 10.00 mmol) was added resulting in a color change to a brown solution. The reaction mixture was refluxed under N_2 atmosphere for 24 h. After 24 h, the reaction was cooled to room temperature and then placed in an ice bath. The reaction was stirred while HCl (30 mL, 1 N) was added dropwise until precipitate formed. After the precipitate formed, the reaction mixture was cooled below 0 °C for 1 h. The precipitate was collected by vacuum filtration and recrystallized in hexanes yielding **10** as light-gray crystals 51% (0.250 g, 1.02 mmol). Mp 110−113 °C; ^{1}H NMR (400 MHz, $CDCl_3$, 25 °C): δ(ppm) 8.06 (s, 1H), 7.91(s, 1H), 7.35 (s, 1H), 6.46 (s, 1H), 2.38 (q, J = 7.6 Hz, 2H), 2.13 (s, 3H), 1.12 (t, J = 7.6, 3H); ^{13}C NMR (100 MHz, $CDCl_3$, 25 °C): δ (ppm) 177.3, 144.5, 142.9, 139.3, 135.0, 134.8, 122.4, 104.0, 16.7, 13.1, 9.7; ^{11}B NMR (sodium tetraphenylborate as standard, 128 MHz, acetone-d_6, 25 °C): δ (ppm) 27.83; IR (ATR) (cm-1): 3346 (w), 3096 (w), 2969 (w), 2939 (w), 2876 (w), 1671 (s), 1628 (w), 1522 (w), 1458 (m), 1384 (s), 1340 (m), 1297 (m), 1162 (m), 1073 (m), 959 (w), 843 (s), 807 (m), 788 (m), 756 (m). HRMS (Magnetic Sector, EI 35 eV) m/z $[M]^{\bullet+}$ calcd for $C_{12}H_{12}BNO_2S$ 245.0682, found 245.0683.

■ ASSOCIATED CONTENT

Supporting Information

The Supporting Information is available free of charge on the ACS Publications website at DOI: 10.1021/acs.joc.6b01998.

X-ray data for **4** (CIF)

X-ray data for **6** (CIF)

^{1}H NMR, ^{13}C NMR, ^{11}B NMR, UV−vis spectra, emission spectra, X-ray data, and further computational details (PDF)

■ AUTHOR INFORMATION

Corresponding Authors

*E-mail: aschrock@uwf.edu

*E-mail: mhuggins@uwf.edu

Notes

The authors declare no competing financial interest.

■ ACKNOWLEDGMENTS

This research was supported by The University of West Florida Office of Undergraduate Research and the Hal Marcus Summer Undergraduate Research Scholarship Program. This work was partially supported by the Mississippi State University Office of Research and Economic Development and the National Science Foundation (OIA-1539035). Computations were performed at the Mississippi State University High Performance Computing Collaboratory and the Mississippi Center for Supercomputing Research.

■ REFERENCES

(1) Yang, X.; Zhao, P.; Qu, J.; Liu, R. *Luminescence* **2015**, *30* (5), 592−599.

(2) Martínez Hardigree, J. F.; Katz, H. E. *Acc. Chem. Res.* **2014**, *47* (4), 1369−1377.
(3) Wang, X.; Liao, Q.; Li, H.; Bai, S.; Wu, Y.; Lu, X.; Hu, H.; Shi, Q.; Fu, H. *J. Am. Chem. Soc.* **2015**, *137* (29), 9289−9295.
(4) Shao, A.; Xie, Y.; Zhu, S.; Guo, Z.; Zhu, S.; Guo, J.; Shi, P.; James, T. D.; Tian, H.; Zhu, W. H. *Angew. Chem., Int. Ed.* **2015**, *54* (25), 7275−7280.
(5) Arbaciauskiene, E.; Kazlauskas, K.; Miasojedovas, A.; Jursenas, S.; Jankauskas, V.; Holzer, W.; Getautis, V.; Sackus, A. *Synth. Met.* **2010**, *160* (5−6), 490−498.
(6) Parkhurst, R. R.; Swager, T. M. *J. Am. Chem. Soc.* **2012**, *134* (37), 15351−15356.
(7) Yang, X.; Xu, X.; Zhou, G. *J. Mater. Chem. C* **2015**, *3* (5), 913−944.
(8) Sekine, C.; Tsubata, Y.; Yamada, T.; Kitano, M.; Doi, S. *Sci. Technol. Adv. Mater.* **2014**, *15* (3), 034203.
(9) Minaev, B.; Baryshnikov, G.; Agren, H. *Phys. Chem. Chem. Phys.* **2014**, *16* (5), 1719−1758.
(10) Guo, X.; Baumgarten, M.; Mullen, K. *Prog. Polym. Sci.* **2013**, *38* (12), 1832−1908.
(11) Doan, P. H.; Pitter, D. R. G.; Kocher, A.; Wilson, J. N.; Goodson, T. *J. Am. Chem. Soc.* **2015**, *137* (29), 9198−9201.
(12) Anthony, J. E. *Chem. Rev.* **2006**, *106* (12), 5028−5048.
(13) Dewar, M. J. S.; Kubba, V. P.; Pettit, R. *J. Chem. Soc.* **1958**, 3073−3076.
(14) Dewar, M. J. S.; Dietz, R. *J. Chem. Soc.* **1959**, 2728−2730.
(15) Dewar, M. J. S.; Kubba, V. P. *Tetrahedron* **1959**, *7* (3), 213−222.
(16) Dewar, M. J. S.; Kubba, V. E. D. P. *J. Org. Chem.* **1960**, *25* (10), 1722−1724.
(17) Dewar, M. J. S.; Kubba, V. P. *J. Am. Chem. Soc.* **1961**, *83* (7), 1757−1760.
(18) Dewar, M. J. S.; Maitlis, P. M. *J. Am. Chem. Soc.* **1961**, *83* (1), 187−193.
(19) Dewar, M. J. S.; Dietz, R. O. Y. *J. Org. Chem.* **1961**, *26* (9), 3253−3256.
(20) Dewar, M. J. S.; Marr, P. A. *J. Am. Chem. Soc.* **1962**, *84* (19), 3782.
(21) Ashe, A. J.; Fang. *Org. Lett.* **2000**, *2* (14), 2089−2091.
(22) Ashe, A. J.; Fang, X.; Fang, X.; Kampf, J. W. *Organometallics* **2001**, *20* (25), 5413−5418.
(23) Pan, J.; Kampf, J. W.; Ashe, A. J. *Organometallics* **2004**, *23* (23), 5626−5629.
(24) Pan, J.; Kampf, J. W.; Ashe, A. J., III *Organometallics* **2008**, *27* (6), 1345−1347.
(25) Marwitz, A. J. V; Abbey, E. R.; Jenkins, J. T.; Zakharov, L. N.; Liu, S.-Y. *Org. Lett.* **2007**, *9* (23), 4905−4908.
(26) Campbell, P. G.; Marwitz, A. J. V; Liu, S. Y. *Angew. Chem., Int. Ed.* **2012**, *51* (25), 6074−6092.
(27) Liu, Z.; Marder, T. B. *Angew. Chem., Int. Ed.* **2008**, *47* (2), 242−244.
(28) Gao, N.; Cheng, C.; Yu, C.; Hao, E.; Wang, S.; Wang, J.; Wei, Y.; Mu, X.; Jiao, L. *Dalton Trans.* **2014**, *43* (19), 7121−7127.
(29) Xiao, J.; Duong, H. M.; Liu, Y.; Shi, W.; Ji, L.; Li, G.; Li, S.; Liu, X. W.; Ma, J.; Wudl, F.; Zhang, Q. *Angew. Chem., Int. Ed.* **2012**, *51* (25), 6094−6098.
(30) Li, G.; Duong, H. M.; Zhang, Z.; Xiao, J.; Liu, L.; Zhao, Y.; Zhang, H.; Huo, F.; Li, S.; Ma, J.; Wudl, F.; Zhang, Q. *Chem. Commun. (Cambridge, U. K.)* **2012**, *48*, 5974−5977.
(31) Oh, J. H.; Lee, H. W.; Mannsfeld, S.; Stoltenberg, R. M.; Jung, E.; Jin, Y. W.; Kim, J. M.; Yoo, J.-B.; Bao, Z. *Proc. Natl. Acad. Sci. U. S. A.* **2009**, *106* (15), 6065−6070.
(32) Xu, C.; Wakamiya, A.; Yamaguchi, S. *J. Am. Chem. Soc.* **2005**, *127* (6), 1638−1639.
(33) Saito, S.; Matsuo, K.; Yamaguchi, S. *J. Am. Chem. Soc.* **2012**, *134* (22), 9130−9133.
(34) Walton, I.; Davis, M.; Munro, L.; Catalano, V. J.; Cragg, P. J.; Huggins, M. T.; Wallace, K. J. *Org. Lett.* **2012**, *14*, 2686−2689.
(35) Boiadjiev, S. E.; Lightner, D. A. *J. Phys. Org. Chem.* **2004**, *17* (8), 675−679.
(36) Boiadjiev, S. E. *ChemInform* **2006**, *38* (9), 349.
(37) Boiadjiev, S. E.; Lightner, D. A. *Monatsh. Chem.* **2008**, *139* (5), 503−511.
(38) Blanksby, S. J.; Ellison, G. B. *Acc. Chem. Res.* **2003**, *36* (4), 255−263.
(39) Grant, D. J.; Dixon, D. A. *J. Phys. Chem. A* **2006**, *110* (47), 12955−12962.
(40) Sugie, M.; Takeo, H.; Matsumura, C. *Chem. Phys. Lett.* **1979**, *64* (3), 573−575.
(41) Yogo, T.; Urano, Y.; Ishitsuka, Y.; Maniwa, F.; Nagano, T. *J. Am. Chem. Soc.* **2005**, *127* (35), 12162−12163.
(42) Oleynik, P.; Ishihara, Y.; Cosa, G. *J. Am. Chem. Soc.* **2007**, *129*, 1842−1843.
(43) Li, M.; Yao, Y.; Ding, J.; Liu, L.; Qin, J.; Zhao, Y.; Hou, H.; Fan, Y. *Inorg. Chem.* **2015**, *54* (4), 1346−1353.
(44) Amstutz, E. D. *J. Org. Chem.* **1952**, *17* (11), 1508−1510.
(45) Jakle, F. *Chem. Rev.* **2010**, *110* (7), 3985−4022.
(46) Zhou, Y.; Xiao, Y.; Li, D.; Fu, M. *J. Org. Chem.* **2008**, *73*, 1571−1574.
(47) Choudhury, A. R.; Mukherjee, S. *Org. Biomol. Chem.* **2012**, *10* (36), 7313−7320.
(48) *Spartan 14*; Wavefunction, Inc.: Irvine, CA, August 28, 2014.
(49) Frisch, M. J.; Trucks, G. W.; Schlegel, H. B.; Scuseria, G. E.; Robb, M. A.; Cheeseman, J. R.; Scalmani, G.; Barone, V.; Mennucci, B.; Petersson, G. A.; Nakatsuji, H.; Caricato, M.; Li, X.; Hratchian, H. P.; Izmaylov, A. F.; Bloino, J.; Zheng, G.; Sonnenberg, J. L.; Hada, M.; Ehara, M.; Toyota, K.; Fukuda, R.; Hasegawa, J.; Ishida, M.; Nakajima, T.; Honda, Y.; Kitao, O.; Nakai, H.; Vreven, T.; Montgomery, J. A., Jr.; Peralta, J. E.; Ogliaro, R.; Bearpark, M.; Heyd, J. J.; Brothers, E.; Kudin, K. N.; Staroverov, V. N.; Kobayashi, R.; Normand, J.; Raghavachari, K.; Rendell, A.; Burant, J. C.; Iyengar, S. S.; Tomasi, J.; Cossi, M.; Rega, N.; Millam, J. M.; Klene, M.; Knox, J. E.; Cross, J. B.; Bakken, V.; Adamo, C.; Jaramillo, J.; Gomperts, R.; Stratmann, R. E.; Yazyev, O.; Austin, A. J.; Cammi, R.; Pomelli, C.; Ochterski, J. W.; Martin, R. L.; Morokuma, K.; Zakrzewski, V. G.; Voth, G. A.; Salvador, P.; Dannenberg, J. J.; Dapprich, S.; Daniels, A. D.; Farkas, O.; Foresman, J. B.; Ortiz, J. V.; Cioslowski, J.; Fox, D. J. *Gaussian 09*, Revision D.01; Gaussian, Inc.: Wallingford, CT, 2009.
(50) Becke, A. D. *J. Chem. Phys.* **1993**, *98*, 5648−5652.
(51) Lee, C.; Yang, W.; Parr, R. G. *Phys. Rev. B: Condens. Matter Mater. Phys.* **1988**, *37*, 785.
(52) Parr, R. G.; Yang, W. *Density Functional Theory of Atoms and Molecules*; Oxford University Press: New York, 1989.
(53) Marques, M. A. L.; Gross, E. K. U. *Annu. Rev. Phys. Chem.* **2004**, *55*, 427−455.
(54) Furche, F.; Ahlrichs, R. *J. Chem. Phys.* **2002**, *117*, 7433−7447.
(55) Furche, F.; Ahlrichs, R. *J. Chem. Phys.* **2004**, *121*, 12772−12773.
(56) Hariharan, P. C.; Pople, J. A. *Theor. Chim. Acta* **1973**, *28*, 213−222.
(57) Hehre, W. J.; Ditchfie, R.; Pople, J. A. *J. Chem. Phys.* **1972**, *56*, 2257−2261.
(58) The 6-31G(d′) basis set has the exponent for the d polarization function for B, C, O, and N taken from the 6-311G(d) basis sets, instead of the value of 0.8 used in the 6-31G(d) basis sets (which had been arbitrarily assigned originally).
(59) Press, W. H. *Numerical recipes: the art of scientific computing*; Cambridge University Press: Cambridge, 1992.

DOI: 10.1021/acs.joc.6b01998
J. Org. Chem. 2016, 81, 10955−10963